ON THE APPLICATION OF CONTINUUM THEORY OF DISLOCATIONS TO THE MECHANICAL BEHAVIOURS OF MULTI-PHASE MATERIALS

Hiroshi Miyamoto* and Masanori Kikuchi*

1. INTRODUCTION

The phase-boundary behaviour of multi-phase materials is an important problem. For example, pile-ups of dislocations occur at grain boundaries of metal polycrystals, and the internal stress field by these performs an important role for the mechanical behaviours of polycrystals. These internal stress fields are considered, from the view point of the continuum theory, due to the incompatibilities at the phase-boundary. So, it is useful to discuss the compatibility conditions. For this purpose, the method of continuum theory of dislocation (CTD) is introduced. The basic idea of this theory is established firstly by Eshelby [1], and Kröner [2] and Mura [3] extended his ideas to many problems.

In this method of CTD, a plastic deformation is considered to occur due to emissions and motions of dislocations. So, an elasto-plastic problem becomes to find out the equilibrium dislocation density, α_{ij}, which satisfies the boundary conditions. This is carried out by using three dimensional elasticity theory. Therefore, an elasto-plastic analysis becomes no other than an elastic analysis. In this paper, analyses are carried out by using finite element method (FEM). If α_{ij} is determined, the internal stress field of these dislocations is determined and the role of the incompatibilities is able to be evaluated.

On the other hand, many studies are carried out for the mechanical behaviours of multi-phase materials by using FEM. In general, a (D^P) matrix method, used for elasto-plastic analyses by FEM, assumes that compatibility conditions are satisfied, so this method is not suitable for the discussion of incompatibilities.

In this paper, two examples of multi-phase materials are analyzed. One is bi-crystal of metal and the other is spherical cast iron. Results are compared with those by a [D^P] matrix method.

2. NUMERICAL PROCEDURE

Assumption is needed for the creation and motion of dislocations which correspond to the plastic deformation. This is made by reference of dislocation theory. Once this is made, distribution of α_{ij} is determined corresponding to a stress field given by elastic analyses by FEM.

*Department of Precision Machinery Engineering, Faculty of Engineering, University of Tokyo.

The determination of equilibrium distribution of α_{ij} is carried out as follows:

(i) By Kröner, relationship between α_{ij} and β^*_{ij}, the plastic distortion tensor, is given as

$$\alpha_{ij} = \varepsilon_{ik\ell}\, \beta^*_{\ell j,k} \ , \tag{1}$$

where, ε_{ijk} is the unit permutation tensor.

(ii) The plastic strain, ε^*_{ij}, is given from plastic distortion tensor as

$$\varepsilon^*_{ij} = (\beta^*_{ij} + \beta^*_{ij})/2 \ . \tag{2}$$

(iii) Owen [4] obtained the internal stress assuming that ε^*_{ij} is equivalent to pre-strain in elastic domain. By FEM, this is carried out by substituting ε^*_{ij} into the following equation.

$$\{F_{in}\} = - \int [B]^T [D] \{\varepsilon^*\} d(vol) \tag{3}$$

where $\{F_{in}\}$ is equivalent nodal force. By $\{F_{in}\}$, internal stress and strain are determined. This consistent to the method of the self-consistent model by Eshelby.

(iv) Examination is performed whether the internal stress is in equilibrium to the dislocation density or not. If it is not, α_{ij} is redetermined by the sum of applied stress and the internal stress and process (iii) is repeated until it reaches the converging value.

(v) In the next stage, load is increased and repeated from procedure (iii).

3. APPLICATION TO THE MECHANICAL BEHAVIOURS OF F.C.C. METAL CRYSTALS

3.1 Assumption

(i) Emission of dislocations occurs when τ_a, the applied shear stress, reaches τ_c, the critical shear stress, until the back stress by emitted dislocations becomes equal to $\tau_a - \tau_c$. Therefore, τ_c on the slipped plane increases to τ_a.

(ii) Relations between the increment of stress, strain and number of dislocations are given by Seeger [5]:

$$d\varepsilon/dn = 9b/16x \ , \tag{4}$$

$$d\sigma = Gbdn/2\Pi L \ , \tag{5}$$

where $d\sigma$, $d\varepsilon$, dn denote the incremental value of stress, strain and number of dislocations, respectively. L is slip line length and x is slip line spacing.

3.2 Single crystal analyses

Figure 1 shows equivalent nodal force obtained by equation (3). Tensile axis is parallel to z-axis. At the free surface, nodal force becomes zero as the free surface condition $\sigma_{ij}n_j = 0$ must be satisfied. Evidently, surface integral of F_i, nodal force, becomes zero.

By the existence of this internal force, the crystal rotates and the deformation of single crystal is not equal all over the area. Figure 2 shows strain distriubtion of single crystals. By [D^P] matrix method, this effect of rotation is not described clearly.

On the other hand, in early stages of deformation of f.c.c. single crystal, many experiments show that only one slip system becomes active. But in this analyses three or four slip systems become active in early stage of deformation. This means that the internal stress of dislocations on primary slip system performs an important role to prevent the activation of other slip systems. Perhaps this occurs at the tip of pile-ups of slip lines as shown in Figure 3(a). But in this analysis, dislocations are assumed to distribute uniformly as in Figure 3(b), therefore, it is difficult to describe these microstructures by this method.

3.3 Bi-crystal analysis

In analyses of bi-crystal, an additional assumption is added that only one ship system among 12 ones is able to be active on which the shear stress (which is the sum of the applied shear stress and the internal shear stress) is the maximum.

Three bi-crystals are analyzed and the tensile axes of which are shown in Figure 4. Figure 5 shows the strain distribution near grain boundaries obtained by a [D^P] matrix method for type C. Strain near grain boundaries varies continuously and smoothly. But the results by CTD varies from Figure 5. Figure 6(a)-(c) show the results obtained by this method. Strain distribution is not smooth near grain boundary. A common feature of the three examples is that the strain parallel to the tensile axis decreases near boundary. In experiments, the decrease of strain near boundary is sometimes observed and these results agree with them, while the result by a [D^P] matrix method is not able to describe this phenomenon.

Moreover, for every type A, B and C the active slip system near boundary is difficult from that far from boundary where the primary slip system is active. At grain boundaries, the phenomena that second slip system becomes active at first is observed. By Chalmers [6] the internal stress field by dislocation pile-ups in one side of bi-crystal provokes slip activations in adjacent crystal. The slip system activated is the one on which sum of the applies stress and the internal stress is the maximum. It is obvious that the method of CTD is able to treat these proceudres analytically, which, by a [D^P] matrix method, is difficult. The state of the variation of shear stresses on first and second slip systems are shown in Table 1 for type C.

4. APPLICATION TO THE MECHANICAL BEHAVIOURS OF SPHERICAL CAST IRON

4.1 Assumption

Emission of dislocations occurs on the plane of the maximum shear stress when τ_a, the maximum shear stress, exceeds τ_c. The number of dislocations

emitted is estimated from the solution by BCS model [7] as

$$n = \frac{\pi(1-\nu)\ell_o}{\mu b}\tau_{eff} \cdot \quad (6)$$

The plastic strain corresponding to the emitted dislocations is determined as follows,

$$\gamma = \frac{1}{2} nb \ , \quad (7)$$

where ℓ_o is the average diameter of crystals and τ_{eff} is $\tau_a - \tau_c$.

Two dimensional analyses are carried out. Figure 7 shows the mesh division for analysis. The black part shows graphite. Volume ratio of graphite (V_g) is 17.1%. Table 2 shows the material constants. The yield stress is employed three kinds of combination. n_R, the ratio of the two is determined as τ_c^g/τ_c^{Fe}, where τ_c^g and τ_c^{Fe} denote the yield stress of graphite and ferrite, respectively.

4.2 Results and discussion

Figure 8(a)-(c) show the propagation states of plastic regions. Black and white region means the plastic region of ferrite and graphite, respectively, and serial numbers of figures express the load stages. The final figurations of plastic zones in ferrite matrix is the same for three n_R values, while they are different distinctly in graphite.

Miyamoto and Oda [8] analyzed the same problem for $n_R = 0.04$ using a [D^P] matrix method. The result is that yield does not occur in graphite. In this analysis, the internal stress of dislocations piled up at the phase boundary is added to the applied stress. Therefore the plastic region of graphite is mainly due to the internal stress fields by the incompatibilities at the phase-boundary. In addition, the direction of propagation of the plastic region in graphite is along the phase-boundary. This corresponds to the result of SEM observation of the fracture surface.

Barnby [9] proposes a model that the fracture of the carbides in an austenitic stainless steel occurs due to the dislocation pile-up at the phase-boundary. The number of dislocations is obtained by one dimensional analysis. In this method, the same considerations are able to be performed. The result for $n_R = 0.081$ is shown in Figure 9. The region of oblique lines shows the region in which dislocations are emitted. Inclinations of lines indicate the slip planes. Dislocation density becomes maximum value ($2.8 \times 10^6/cm^2$) at point a and becomes minimum ($2.0 \times 10^4/cm^2$) at point b. In Figure 10(a) and (b), the equivalent nodal force is represented for $n_R = 0.04$ and 0.081. Comparing the two cases, it is noticed that the equivalent nodal forces for $n_R = 0.04$ are smaller than those for $n_R = 0.081$. It is reasonable that for $n_R = 0.04$ yielding occurs in graphite, while for $n_R = 0.081$ it is not observed until final stage of analyses. That is, for $n_R = 0.04$, stresses of dislocations are released at phase-boundary.

4. DISCUSSION

By Ashby [10], dislocations in non-homogeneous materials are divided into two parts, one is statistically-stored dislocations, ρ_s, which corresponds to a general, uniform deformation and the other is geometrically-stored

dislocations, ρ_g, which corresponds to a local, non-uniform deformation. In this paper, ρ_g is mainly considered, and the results show that the method of CTD is useful to discuss the effect of ρ_g. But about ρ_s, it is difficult to describe the actual physical phenomenon accurately (see equations (4) and (6)). The difficulties occurred in single crystal analyses are due to this fact. So, it is necessary to develop this method combining with the experimental studies.

5. SUMMARY

(i) The method of CTD is intorudced to discuss the effect of incompatibilities at the phase-boundary. By this method an elasto-plastic analysis becomes an elastic analysis.
(ii) Mechanical behaviours of f.c.c. metal crystals are analysed by CTD. The effect of dislocation pile-ups is able to be evaluated, while it is difficult by a [D^P] matrix method.
(iii) Spherical cast iron is also analyzed. Considerations similar to that of Barnby is carried out two-dimensionally.
(iv) It becomes obvious that this method is very useful to know about ρ_g, but about ρ_s, many experimental studies are needed.

ACKNOWLEDGEMENT

Authors with to thank Mr. Yoshito Mitani, post graduate student of the University of Tokyo, for his valuable comments and discussions.

REFERENCES

1. ESHELBY, J. D., Phil. Trans. A, 244, 1957, 87.
2. KRÖNER, E., Kontinuums Theorie der Versetzungen und Eigenspannungen, Springer Verlag, Berlin, 1958.
3. MURA, T., Inealstic Behaviours of Solids, 1970, 211.
4. OWEN, D. R. J., Journal for Numerical Methods in Engineering, Vol. 9, 1973.
5. SEEGER, A., KRÖNMULLER, H., MADER, S. and TRAUBLE, H., Phil. Mag. 6, 1961, 639.
6. CHALMERS, B. and LIVINGSTON, J. D., Acta. Met, 5, 1957, 322.
7. BILBY, B. A., COTTRELL, A. H. and SWINDEN, K. H., Proc. Roy. Soc. A, 272, 1964, 304.
8. MIYAMOTO, H. and ODA, J., Preprint of JSME 760-2.
9. BARNBY, J. T., Acta. Met. 15, 1967, 903.
10. ASHBY, M. F., Phil. Mag., 19, 1970, 399.

Table 1 Comparison of shear stress for type C

SHEAR STRESS (MPa)		
LOAD STAGE	PRIMARY SLIP SYSTEM $(\bar{1}\bar{1}1)$ $[\bar{1}10]$	SECONDARY SLIP SYSTEM $(\bar{1}11)$ $[o1\bar{1}]$
1	-2.26	2.19
2	-2.49	2.42
3	-2.56	2.54
4	-2.58	2.63
5	-2.59	2.71
6	-2.60	2.80

Table 2 Material constants

	FERITE	GRAPHITE
E (MPa)	205800.0	4900.0
ν	0.29	0.16
τ_c (MPa)		
$n_R = 0.04$	490.0	19.6
$n_R = 0.06$	490.0	29.4
$n_R = 0.081$	362.6	29.4

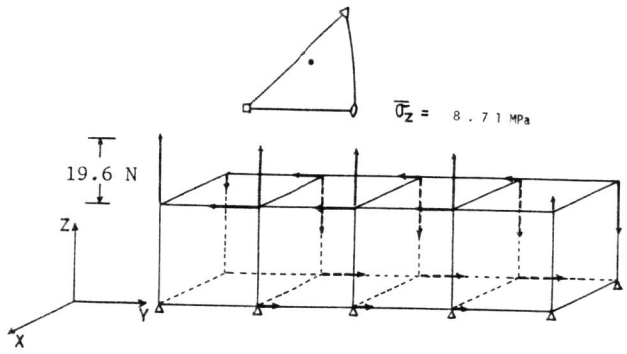

Figure 1

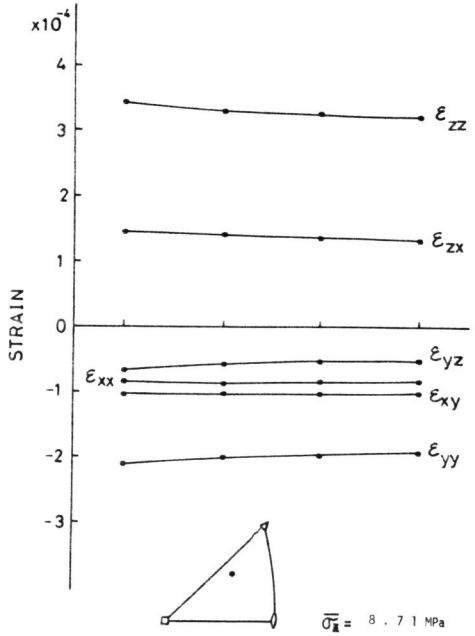

Figure 2 Strain distribution of single crystal

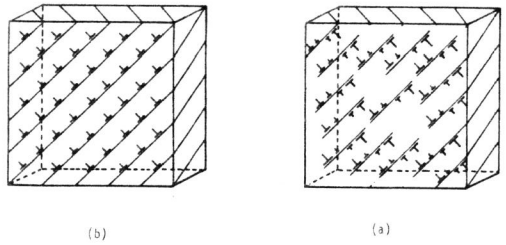

Figure 3

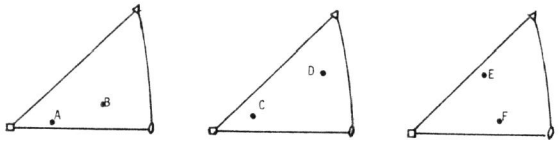

Figure 4 Tensile axes of three kinds of bi-crystals

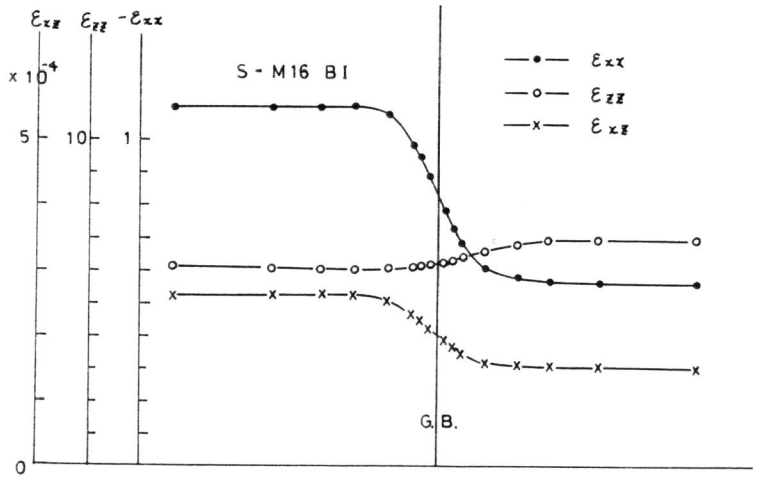

Figure 5 Strain distribution of bi-crystal by a $[D^P]$ matrix method

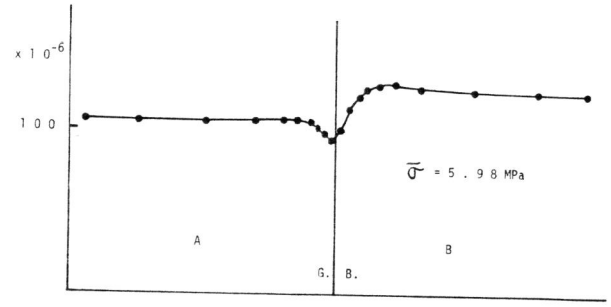

Fig.6 (a) For type A

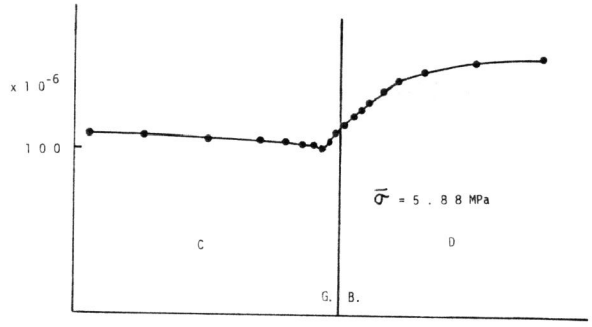

Fig.6 (b) For type B

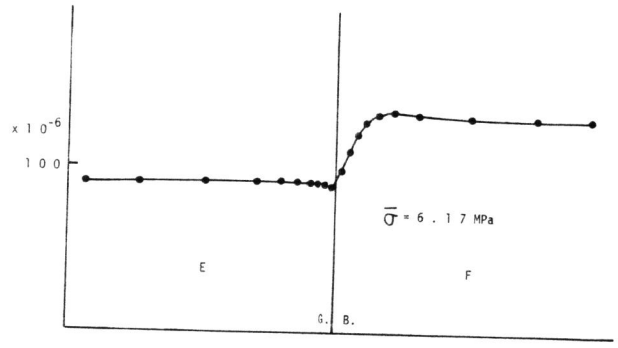

Fig.6 (c) For type C

Figure 6 Strain distribution near grain boundary

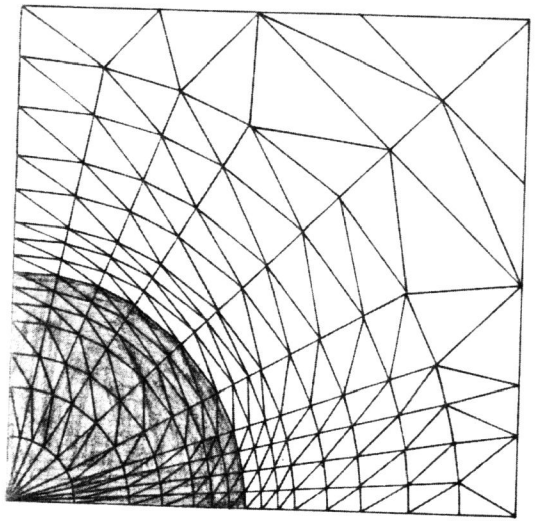

Figure 7 Mesh division of spheroidal cast iron

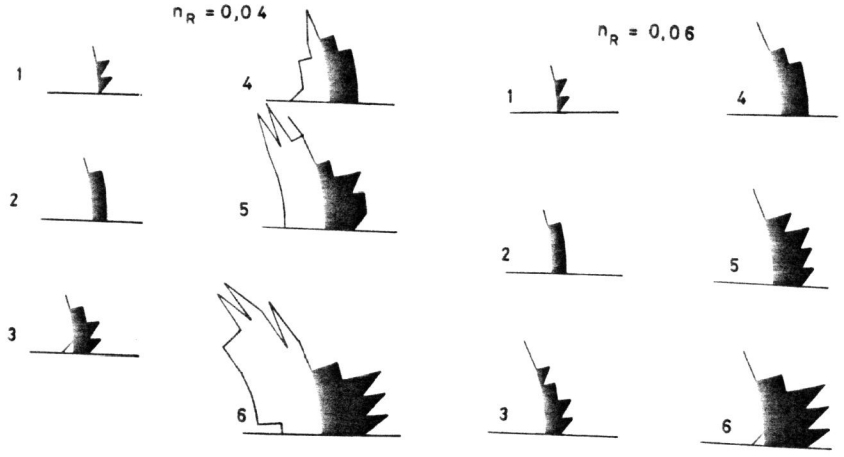

(a) (b)

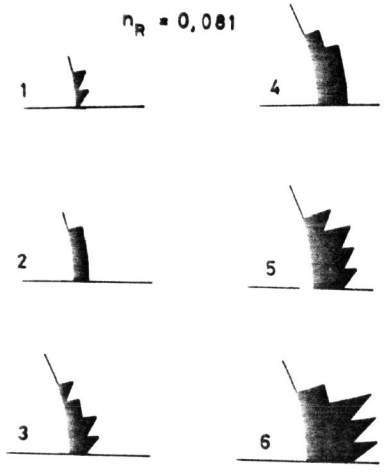

(c)

Figure 8 Propagation states of plastic region for three n_R

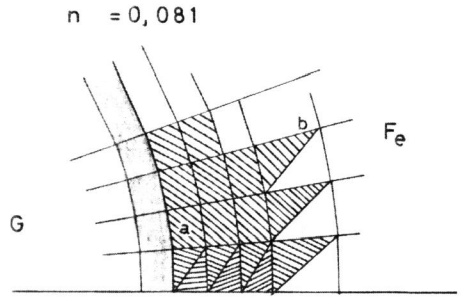

Figure 9

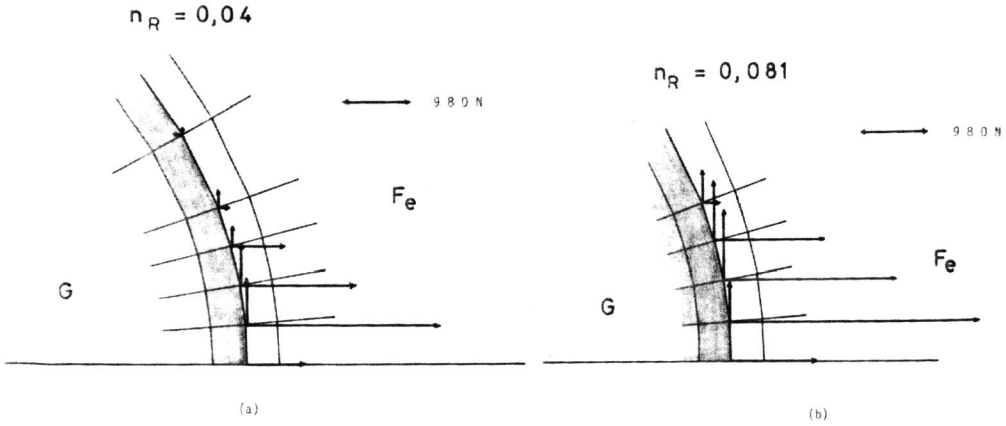

Figure 10